CHAPTER W14

Polymers

W14.1 Structure of Ideal Linear Polymers

The first quantity characterizing the polymer is the molecular weight. If M_1 is the mass of a monomer unit, the mass of the polymer molecule is

$$M_{N+1} = (N+1)M_1. \tag{W14.1}$$

Often, there will be a distribution of values of N in a macroscopic sample, so there will be a distribution of masses. We return to this point later.

If one were to travel along the polymer from end to end, one would travel a distance Na, where a is the length of a monomer unit. The end-to-end distance in space, however, would be shorter than this, due to the contorted shape of the polymer. The mean-square end-to-end distance $\langle r_N^2 \rangle$ of a polymer with N intermonomer bonds may be calculated. Figure W14.1 shows a chain in which the monomer units are labeled $0, 1, 2, \ldots, N$. One endpoint is at 0 and the other is at N. The vector from monomer 0 to monomer n is denoted by $\mathbf{r}_n$. Thus $\mathbf{r}_0 = \mathbf{0}$, the null vector, whereas $\mathbf{r}_N$ is the end-to-end vector. The vector from monomer m to monomer $m+1$ is denoted by $a\hat{u}_{m+1}$, where $\{\hat{u}_j,\ j = 1, 2, \ldots, N\}$ are a set of unit vectors.

In the ideal polymer it will be assumed that these unit vectors are uncorrelated with each other, so that if an ensemble average were performed,

$$\langle \hat{u}_j \rangle = 0 \quad \text{and} \quad \langle \hat{u}_j \cdot \hat{u}_k \rangle = \delta_{j,k}, \tag{W14.2}$$

where $\delta_{j,k} = 0$ or 1, depending on whether $j \neq k$ or $j = k$, respectively. It follows that

$$\mathbf{r}_N = \sum_{n=1}^{N} a\hat{u}_n, \tag{W14.3}$$

$$r_N^2 = a^2 \sum_{n=1}^{N} \sum_{m=1}^{N} \hat{u}_m \cdot \hat{u}_n. \tag{W14.4}$$

Performing an ensemble average yields

$$\langle \mathbf{r}_N \rangle = 0, \tag{W14.5}$$

$$\langle r_N^2 \rangle = a^2 \sum_{n=1}^{N} \sum_{m=1}^{N} \langle \hat{u}_m \cdot \hat{u}_n \rangle = a^2 \sum_{n=1}^{N} \sum_{m=1}^{N} \delta_{m,n} = a^2 \sum_{n=1}^{N} 1 = Na^2. \tag{W14.6}$$

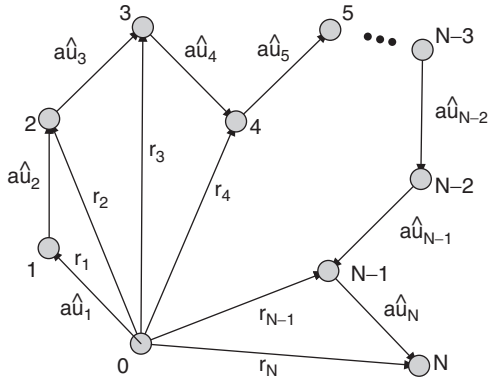

Figure W14.1. Structure of an ideal linear polymer chain.

One may also look at the shadows of the vector $\mathbf{r}_N$ on the yz, xz, and xy planes. Denote these by x_N, y_N, and z_N, respectively. It follows that

$$\langle x_N \rangle = \langle y_N \rangle = \langle z_N \rangle = 0. \tag{W14.7}$$

Due to the isotropy of space, it also follows that the mean-square end-to-end shadow distances (ETESDs) are

$$\langle x_N^2 \rangle = \langle y_N^2 \rangle = \langle z_N^2 \rangle = \tfrac{1}{3}\langle x_N^2 + y_N^2 + z_N^2 \rangle = \tfrac{1}{3}\langle r_N^2 \rangle = \tfrac{1}{3}Na^2. \tag{W14.8}$$

For an ensemble of polymers there will be a distribution of end-to-end distances. This distribution may be found from a simple symmetry argument. Let $F_N(x_N^2)dx_N$ be the probability for finding the ETESD within a bin of size dx_N at $x = x_N$. This may be written as an even function of x_N since there is nothing to distinguish right from left in the problem. The probability for finding the vector $\mathbf{r}_N$ in volume element $dV = dx_N\, dy_N\, dz_N$ is

$$dP = F(x_N^2)F(y_N^2)F(z_N^2)\, dV = G(r_N^2)\, dV, \tag{W14.9}$$

where, by the isotropy of space, dP can depend only on the magnitude of r_N. Here $G_N(r_N^2)\, dV$ gives the probability for finding the end-to-end distance in volume element dV. If the relation above is differentiated with respect to x_N^2, the result is

$$F'(x_N^2)F(y_N^2)F(z_N^2) = G'(r_N^2). \tag{W14.10}$$

Dividing this by

$$F(x_N^2)F(y_N^2)F(z_N^2) = G(r_N^2) \tag{W14.11}$$

results in

$$\frac{F'(x_N^2)}{F(x_N^2)} = \frac{G'(r_N^2)}{G(r_N^2)}. \tag{W14.12}$$

Since r_N may be varied independently of x_N (e.g., by varying y_N), both sides of this equation must be equal to a constant. Call this constant $-\alpha_N$. Integrating the resulting first-order differential equation produces

$$F_N(x_N^2) = A_N e^{-\alpha_N x_N^2}. \tag{W14.13}$$

Since this represents a probability it must be normalized to 1, that is,

$$1 = \int_{-\infty}^{\infty} F_N(x_N^2)\, dx_N = \int_{-\infty}^{\infty} A_N e^{-\alpha_N x_N^2}\, dx_N = A_N \sqrt{\frac{\pi}{\alpha_N}}, \tag{W14.14}$$

so $A_N = (\alpha_N/\pi)^{1/2}$.

Use this probability distribution, F_N, to compute $\langle x_N^2 \rangle$:

$$\langle x_N^2 \rangle = \int_{-\infty}^{\infty} \sqrt{\frac{\alpha_N}{\pi}} x_N^2 e^{-\alpha_N x_N^2}\, dx_N = \frac{1}{2\alpha_N} = \frac{Na^2}{3}, \tag{W14.15}$$

where the last equality follows from Eq. (W14.8). Thus

$$F_N(x_N^2) = \left(\frac{3}{2\pi N a^2}\right)^{1/2} e^{-3x_N^2/2Na^2}, \tag{W14.16}$$

$$G_N(r_N^2) = \left(\frac{3}{2\pi N a^2}\right)^{3/2} e^{-3r_N^2/2Na^2}. \tag{W14.17}$$

A plot of the end-to-end distance probability distribution function as a function of $\rho = r/a\sqrt{N}$ is given in Fig. W14.2. In this graph the volume element has been written as $4\pi r_N^2\, dr_N$. Note that the most probable value of r is $a(2N/3)^{1/2}$, as may be verified by finding the extremum of the curve. This $N^{1/2}$ dependence is characteristic of processes involving a random walk of N steps.

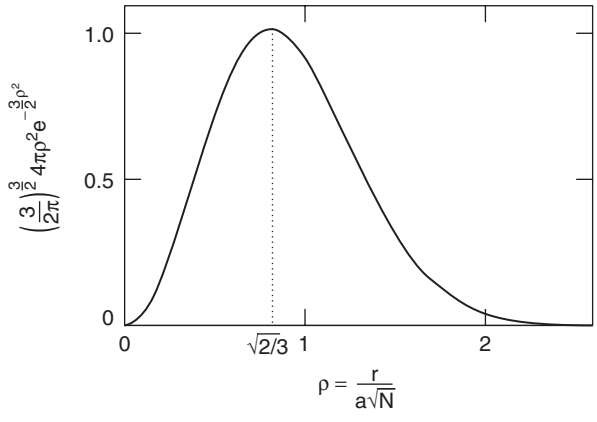

Figure W14.2. End-to-end distance probability distribution $G_N(R_N^2)$ for the ideal linear polymer.

The center of mass of the polymer is defined (approximately, by neglecting end-group corrections) by

$$\mathbf{R} = \frac{1}{N+1}\sum_{n=0}^{N} \mathbf{r}_n. \tag{W14.18}$$

Let $\mathbf{s}_n$ be the location of the nth monomer relative to the center of mass:

$$\mathbf{s}_n = \mathbf{r}_n - \mathbf{R}. \tag{W14.19}$$

Define a quantity s^2 that is the mean square of s_n:

$$s^2 \equiv \frac{1}{N+1}\sum_{n=0}^{N} \langle s_n^2 \rangle. \tag{W14.20}$$

In the polymer literature the parameter s is referred to as the *radius of gyration*, although its definition conflicts with that used in the mechanics of rigid bodies. Thus

$$\sum_{n=0}^{N} \langle s_n^2 \rangle = \sum_{n=0}^{N} \langle (\mathbf{r}_n - \mathbf{R})^2 \rangle = \sum_{n=0}^{N} \langle r_n^2 \rangle - (N+1)\langle R^2 \rangle. \tag{W14.21}$$

Note that

$$\sum_{n=0}^{N} \langle r_n^2 \rangle = \sum_{n=0}^{N} na^2 = \frac{N(N+1)}{2}a^2. \tag{W14.22}$$

Also

$$\langle R^2 \rangle = \left(\frac{1}{N+1}\right)^2 \sum_{m=1}^{N}\sum_{n=1}^{N} \langle \mathbf{r}_n \cdot \mathbf{r}_m \rangle. \tag{W14.23}$$

Note that

$$\langle \mathbf{r_n} \cdot \mathbf{r_m} \rangle = a^2 \sum_{j=1}^{n}\sum_{k=1}^{m} \langle \hat{u}_j \cdot \hat{u}_k \rangle = a^2 \sum_{j=1}^{n}\sum_{k=1}^{m} \delta_{j,k} = a^2 \min(m, n), \tag{W14.24}$$

where $\min(m, n) = m$ when $m < n$, and vice versa. It follows that

$$\begin{aligned}
\langle R^2 \rangle &= \frac{1}{(N+1)^2}\sum_{n=1}^{N}\sum_{m=1}^{N} a^2 \min(m, n) = \left(\frac{a}{N+1}\right)^2 \sum_{n=1}^{N}\left(\sum_{m=1}^{n} m + \sum_{m=n+1}^{N} n\right) \\
&= \left(\frac{1}{N+1}\right)^2 \sum_{n=1}^{N}\left[\frac{n(n+1)}{2} + n(N-n)\right] \\
&= \left(\frac{a}{N+1}\right)^2 \frac{N}{6}(2N^2 + 3N + 1) = \frac{a^2}{6}\frac{N}{N+1}(2N+1).
\end{aligned} \tag{W14.25}$$

For large N this approaches

$$\langle R^2 \rangle \approx \frac{Na^2}{3}. \tag{W14.26}$$

By coincidence, this is the same as the expression given in Eq. (W14.15). An expression for the square of the radius of gyration is finally obtained:

$$s^2 = \frac{a^2}{6}\frac{N(N+2)}{N+1} \longrightarrow N\frac{a^2}{6}. \tag{W14.27}$$

It is also possible to obtain a formula for the mean-square distance of a given monomer to the center of mass:

$$\langle s_n^2 \rangle = \langle r_n^2 \rangle - 2\langle \mathbf{R} \cdot \mathbf{r}_n \rangle + \langle R^2 \rangle. \tag{W14.28}$$

Using

$$\langle \mathbf{R} \cdot \mathbf{r}_n \rangle = \frac{a^2}{N+1}\left(\sum_{m=1}^{n} m + \sum_{m=n+1}^{N} n\right) = \frac{a^2}{N+1}\left[-\frac{n^2}{2} + n\left(N + \frac{1}{2}\right)\right] \tag{W14.29}$$

results in

$$\langle s_n^2 \rangle = \frac{N^2a^2}{N+1}\left\{\frac{1}{3}[w^3 + (1-w)^3] + \frac{1}{6N}\right\} \longrightarrow N\frac{a^2}{3}[w^3 + (1-w)^3], \tag{W14.30}$$

where $w = n/N$.

Finally, the symmetry argument employed previously may be used to obtain an expression for the probability distribution function, $P(s_n)$, for the distances s_n. Isotropy of space leads to a Gaussian functional form for P:

$$P(s_n) = Ae^{-\gamma s_n^2}. \tag{W14.31}$$

Using this to evaluate $\langle s_n^2 \rangle$ leads to the expression

$$\langle s_n^2 \rangle = \frac{\int d^3s_n s_n^2 \exp(-\gamma s_n^2)}{\int d^3s_n \exp(-\gamma s_n^2)} = \frac{3}{2\gamma} = N\frac{a^2}{3}\left[\left(\frac{n}{N}\right)^3 + \left(1 - \frac{n}{N}\right)^3\right], \tag{W14.32}$$

so

$$\gamma = \frac{9}{2}\left(\frac{N}{a}\right)^2 \frac{1}{n^3 + (N-n)^3}, \tag{W14.33}$$

$$A = \left(\frac{\gamma}{\pi}\right)^{3/2}. \tag{W14.34}$$

W14.2 Self-Avoiding Walks

There are two constraints that a linear-chain polymer must obey: each monomer must be attached to the previous monomer in the chain, and no monomer can cross another monomer. The case of a single molecule is considered first, followed by a dense collection of molecules. If only the first constraint is imposed, the result has already been derived: the end-to-end distance grows as $\sqrt{N}$, just as in a random walk. It will be seen that the effect of the second constraint is to transform this to $r_N \propto N^{\nu}$, where $\nu = 0.588 \pm 0.001$. The fact that the distance grows as a power of N greater than that for the overlapping chain model is expected. After all, since certain back-bending configurations are omitted because they lead to self-overlap, it is expected that the chain will form a looser, more-spread-out structure. The precise value of the exponent depends on the results of a more detailed calculation.

In Table W14.1, results are presented for a random walk on a simple cubic lattice. For a walk of N steps, starting at the origin, there are 6^N possible paths. The 6 comes from the fact that at each node there are six possible directions to go: north, south, east, west, up, or down. The table presents the number of self-avoiding walks and also the mean end-to-end distance. The exponent may be estimated by a simple argument. At the simplest level ($N = 2$) the effect of nonoverlap is to eliminate one of the six possible directions for the second step (Fig. W14.3). The mean end-to-end distance is therefore $(2 + 4\sqrt{2})/5 = 1.531371\ldots$. For a polymer of length N, imagine that it really consists of two polymers of length $N/2$. These two half-polymers are assumed to combine with the same composition rule as the two one-step segments above did. Assuming the scaling formula $r_N = AN^{\nu}$, one obtains

$$AN^{\nu} = A\left(\frac{N}{2}\right)^{\nu} \frac{2 + 4\sqrt{2}}{5}, \tag{W14.35}$$

which leads to $\nu = 0.6148237\ldots$. Successive refinements of the exponent are obtained by applying the scaling prescription above to the entries in Table W14.1. Acceleration of the convergence of the exponent is obtained by averaging successive values of the exponents.

TABLE W14.1 Self-Avoiding Walks on a Cubic Lattice

Number of Steps N	Number of Possible Paths n (paths)	Number of Self-Avoiding Paths of Length N n (SAW paths)	Mean End-to-End Distance $\langle s \rangle$
1	6	6	1.00000
2	36	30	1.53137
3	216	150	1.90757
4	1,296	726	2.27575
5	7,776	3,534	2.57738
6	46,656	16,926	2.88450
7	279,936	81,390	3.14932
8	1,679,616	387,966	3.42245
9	10,077,696	1,853,886	3.62907
10	60,466,176	8,809,878	3.89778

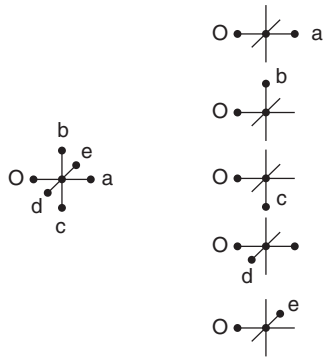

Figure W14.3. A polymer "path" starts at O and after two steps ends up at positions a, b, c, d, or e. Path $O-a$ has length 2; the other paths have length $\sqrt{2}$.

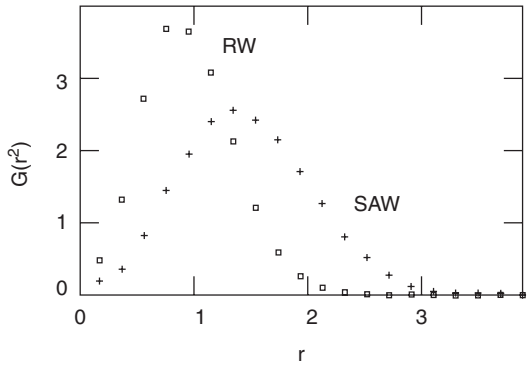

Figure W14.4. Comparison of the end-to-end distance distributions $G(r^2)$ for the random walk (RW) and the self-avoiding walk (SAW). The units are arbitrary.

In Fig. W14.4 the distribution of end-to-end distances for the random walk (RW) is compared to the distribution of distances for the self-avoiding walk (SAW). The curves were generated by constructing a chain of 100 spheres, with each successive sphere touching the previous one at a random location. An ensemble average of 10,000 random chains was made. One verifies that the SAW distribution is more extended than the RW distribution.

Next consider a dense polymer. Each monomer is surrounded by other monomers, some belonging to its own chain and some belonging to others. The no-crossing rule applies to all other monomers. By extending the chain to larger sizes, the chain will avoid itself, but it will more likely overlap other chains. Thus there is nothing to gain by having a more extended structure. The net result is that there is a cancellation effect, and the chain retains the shape of a random walk. Thus in the dense polymer the mean end-to-end distance grows as $\sqrt{N}$.

W14.3 Persistence Length

On a large-enough length scale, a long polymer molecule will look like a random curve. On a short-enough length scale, however, a segment of the polymer may look straight.

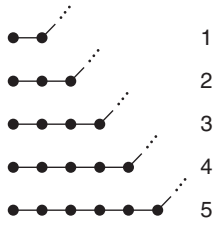

Figure W14.5. Various possible bend locations in a polymer.

The question is at what length scale the transition occurs. The characteristic distance is called the *persistence length*, L_p. A simple statistical argument provides an estimate of this length. Refer to Fig. W14.5 to see the enumeration of bending configurations.

Select a monomer at random and look at its NN and subsequent neighbors down the chain. Let p be the probability that two neighboring bonds are not parallel to each other and $q = 1 - p$ be the probability that they are parallel to each other. The probability of forming a bend after moving one monomer down the chain is $P_1 = p$. The probability of forming the first bend after traversing two bonds is $P_2 = qp$. Similarly, the probability of traversing n bonds before the bend is

$$P_n = q^{n-1}p. \tag{W14.36}$$

Note that the probability is properly normalized, since

$$\sum_{n=1}^{\infty} P_n = \sum_{n=1}^{\infty} (1-p)^{n-1}p = \frac{p}{1-(1-p)} = 1. \tag{W14.37}$$

The mean number of parallel bonds before a bend occurs is

$$\langle n \rangle = \sum_{n=1}^{\infty} P_n n = \frac{p}{q}\sum_{n=1}^{\infty} nq^n = p\frac{\partial}{\partial q}\frac{1}{1-q} = \frac{1}{p}. \tag{W14.38}$$

The persistence length is obtained by multiplying this by the bond length, a:

$$L_p = \frac{a}{p}. \tag{W14.39}$$

Suppose that the bend formation requires an activation energy E_b and that there are g possible ways of making the bend. Then

$$p = \frac{ge^{-\beta E_b}}{1 + ge^{-\beta E_b}} \approx ge^{-\beta E_b}, \tag{W14.40}$$

where it is assumed that $E_b \gg k_B T$. Thus

$$L_p = \frac{a}{g}e^{\beta E_b}. \tag{W14.41}$$

At low temperatures the persistence length of an isolated polymer will be long. At high temperatures L_p becomes shorter. This assumes, of course, that there are no obstacles in the way to prevent coiling and uncoiling of the polymer. In a dense polymer melt, however, the steric hindrance due to the presence of the other molecules prevents this coiling–uncoiling from occurring.

W14.4 Free-Volume Theory

The concept of packing fraction has already been encountered when analyzing crystalline order and the random packing of hard spheres. The same concept carries over to the case of polymers. When the polymer is below the melting temperature, T_m, and is cooled, it contracts by an amount determined by the volume coefficient of thermal expansion, β. Consistent with a given volume there are many possible configurations that a polymer molecule may assume. As the temperature is lowered closer to the glass-transition temperature, T_g, the volume shrinks further and the number of possible configurations is reduced. Concurrent with the decrease of volume and reduction in the number of configurations is a rapid increase in the viscosity of the polymer. These trends may be related by introducing the free-volume theory, or the closely related configurational-entropy approach.

Free volume is defined as the difference in the volume that a sample has and the volume it would have had if all diffusion processes were to cease. Recall that at $T = 0$ K all thermal motion ceases. For low temperatures, atomic vibrational motion occurs, but the atoms retain their mean center-of-mass positions. Below the Kauzmann temperature, T_K, all atoms on a polymer chain are sterically hindered by other atoms and there can be no diffusion of the individual atoms on the polymer chain. At a temperature above the Kauzmann temperature there can be some diffusion of the atoms comprising the polymer, but the polymer as a whole still cannot move, since some of its atoms are pinned by the steric hindrance of other atoms. It is not until a temperature $T_g > T_K$ is reached that the molecule as a whole may begin to move. This motion usually involves the concerted motion of a group of atoms. For the group of atoms to diffuse, there must be a space for it to move into. The free volume is a measure of that space. It is important to distinguish free volume from void space. In both the crystalline state and the random close-packed structure there is void space but no free volume. If PF is the packing fraction, $1 - \text{PF}$ is a measure of that void space. Free volume begins to form when the volume constraint on the system is relaxed and the atoms are permitted some "breathing room." The packing fraction when there is free volume is $f < \text{PF}$. Free volume plays the same role in amorphous polymers as vacancies play in crystals.

Imagine that the polymers are partitioned into molecular groups (i.e., groups of atoms on the polymer chain that are free to diffuse above T_K). It will be assumed that this distribution costs no energy, the partitioning being based just on probabilities. Let V_f be the total free volume available to a system of N such molecular groups. The average free volume per molecular group is

$$v_f = \frac{V_f}{N}. \tag{W14.42}$$

Imagine that the free volume available to a molecular group comes in various sizes, which will be labeled v_i. Let N_i be the number of groups assigned the volume v_i. Then

there are two constraints:

$$\sum_i N_i = N \tag{W14.43}$$

and (neglecting possible overlaps of free volume)

$$\sum_i N_i v_i = V_f. \tag{W14.44}$$

The number of ways to partition N molecular groups into classes with N_1 in the first class, N_2 in the second class, and so on, is given by the multinomial coefficient W:

$$W = \frac{N!}{N_1!N_2!\cdots} = \frac{N!}{\prod_i N_i!}. \tag{W14.45}$$

The most probable distribution is sought [i.e., the one with the maximum configurational entropy, $S = k_B \ln(W)$]. This involves maximizing W subject to the two prior constraints. First use Stirling's approximation, $\ln(N!) \approx N\ln(N) - N$, to write

$$\ln(W) = N\ln(N) - N - \sum_i [N_i \ln(N_i) - N_i]. \tag{W14.46}$$

When $\ln(W)$ is maximized with respect to the N_i, W will also be maximized. Introduce Lagrange multipliers γ and λ to maintain these constraints and vary the quantity $\ln(W) - \gamma\left(\sum N_i - N\right) - \lambda\left(\sum N_i v_i - V_f\right)$ with respect to the variables N_i, to obtain

$$\frac{\partial}{\partial N_i}\left\{N\ln(N) - N - \sum_i [N_i \ln(N_i) - N_i] - \gamma\left(\sum_i N_i - N\right)\right.$$
$$\left. -\lambda\left(\sum_i N_i v_i - V_f\right)\right\} = 0, \tag{W14.47}$$

so

$$-\ln(N_i) - \gamma - \lambda v_i = 0. \tag{W14.48}$$

Solving this for the probability of obtaining a given volume yields

$$p_i = \frac{\exp(-\lambda v_i)}{\sum_i \exp(-\lambda v_i)}. \tag{W14.49}$$

The value of λ is fixed by the constraint

$$v_f = \sum_i p_i v_i = -\frac{\partial}{\partial \lambda} \ln \sum_i \exp(-\lambda v_i). \tag{W14.50}$$

A further approximation is called for. Introduce a volume density of states

$$\rho(v) = \sum_i \delta(v - v_i) \tag{W14.51}$$

and write

$$\sum_i \exp(-\lambda v_i) = \int \rho(v) \exp(-\lambda v)\, dv. \tag{W14.52}$$

It will be assumed that the volume density of states may be approximated by a constant, although other possible variations may be imagined. Then

$$\sum_i \exp(-\lambda v_i) = \int_0^\infty \rho_0 \exp(-\lambda v)\, dv = \frac{\rho_0}{\lambda}, \tag{W14.53}$$

and $v_f = 1/\lambda$.

The next assumption involves arguing that motion of a molecular group cannot occur until a minimum amount of free volume, v^*, is assigned to it. The probability for having $v > v^*$ is

$$p^* = \sum_i p_i \Theta(v_i - v^*) = \frac{\displaystyle\int_{v^*}^\infty \rho(v) \exp(-v/v_f)\, dv}{\displaystyle\int_0^\infty \rho(v) \exp\left(-\frac{v}{v_f}\right) dv} = \exp\left(-\frac{v^*}{v_f}\right). \tag{W14.54}$$

Recall from elementary physics that a hole in a solid expands when the solid expands. This concept applies to the free volume as well, so

$$\frac{dv_f}{dT} = \beta(v_f + v_K), \tag{W14.55}$$

where β is the volume thermal-expansion coefficient and v_K is the volume per molecular group at the Kauzmann temperature, T_K. Integrating this, and assuming for simplicity's sake that β is constant, leads to

$$v_f(T) = v_K(e^{\beta(T-T_K)} - 1) \approx v_K \beta (T - T_K), \tag{W14.56}$$

where it is assumed that the exponent is small enough to be linearized. Thus

$$p^* = \exp\left[-\frac{v^*}{v_K \beta (T - T_K)}\right]. \tag{W14.57}$$

By assumption, the viscosity η varies inversely as p^*. Normalize it to the value η_g, the viscosity at temperature T_g:

$$\frac{\eta(T)}{\eta_g} = \exp\left[\frac{v^*}{v_K \beta}\left(\frac{1}{T - T_K} - \frac{1}{T_g - T_K}\right)\right]. \tag{W14.58}$$

This leads to the Williams–Landel–Ferry (WLF) equation

$$\log_{10} \frac{\eta(T)}{\eta_g} = -\frac{C_1(T - T_g)}{C_2 + T - T_g}. \tag{W14.59}$$

Empirically, it is found that $C_1 = 17.4$ and $C_2 = T_g - T_K = 51.6$ K are the average values for many polymers. This means that the glass-transition temperature is on the average about 51.6 K above the Kauzmann temperature. Also, the free volume at the glass-transition temperature amounts to 2.5% of the critical volume for diffusion:

$$v_{f,g} = v_k \beta (T_g - T_K) = \frac{v^*}{C_1} \log_{10} e = 0.025\ v^*. \tag{W14.60}$$

The time–temperature superposition principle presupposes the existence of a universal connection between viscosity and temperature. The WLF formula shows that this supposition is, in fact, warranted. The free-volume theory also predicts that diffusion of gases through the polymer should increase considerably above T_K and should increase further above T_g. It also predicts that the application of pressure, which compresses the material and hence removes free volume, should serve to increase the viscosity. This prediction is consistent with experiment.

One may measure the free volume by relating it to the thermal expansion of the solid. Write the total volume of a sample at temperature T as the sum of three terms, $V(T) = V_p + V_v + V_f$, where V_p is the volume occupied by the polymer atoms, V_v is the void space, and $V_f(T)$ is the free volume. At $T = T_g$, $V_f(T_g) = 0$ and $V(T_g) = V_p + V_v \equiv V_g$. For $T > T_g$, $V(T) = V_g[1 + \beta(T - T_g)]$. Then $V_f(T) = V_g \beta (T - T_g)$. In practice one takes for β the difference in the values of the volume coefficient of thermal expansion above and below T_g.

Note that the distinction between T_K and T_g really exists only for macromolecules such as polymers. For small molecules the movement of individual atoms is tantamount to the motion of the molecule as a whole.

It is now believed that free-volume theory was a useful milestone in the approach to a full understanding of the glass transition but is not the ultimate explanation. Modern advances in what is known as mode-coupling theory provide a more fundamental approach toward this understanding.

W14.5 Polymeric Foams

Foams constructed from polymers offer a variety of uses, including filters, supports for catalysts and enzymes, and possible applications as electrodes in rechargeable batteries. Examples range from polyurethane cushions to polystyrene coffee cups. Here the focus is on one example of such a foam made of cross-linked polystyrene. Most of this material consists of empty space, with the void volume typically occupying more than 90% of the total. There is a fully interconnected network of empty chambers connected by holes whose size can vary between 2 and 100 μm in diameter, with a fairly uniform size distribution (±20%). The density is typically in the range 20 to 250 kg/m^3.

The foam is created by an emulsion technique that combines water, oil (containing styrene), and an emulsifier, followed by vigorous agitatation of the mixture. The emulsifier keeps the small oil droplets formed from recombining into larger droplets. The water droplets can be made to occupy more than the 74% needed to form a close-packed structure of uniform spheres by including additional smaller droplets. The emulsion resembles soap bubbles, but with the air being replaced by water (Fig. W14.6). Persulfates are present as an initiator for the polymerization and divinylbenzene serves as the cross-linker as in the vulcanization process discussed

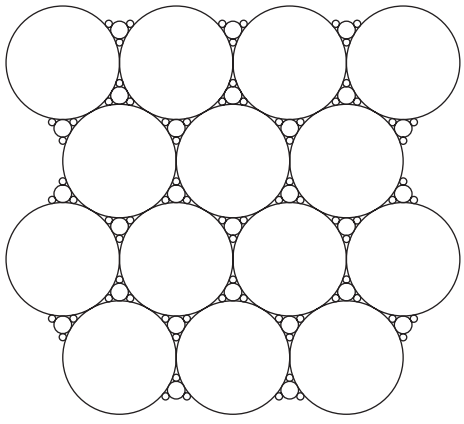

Figure W14.6. Two-dimensional representation of a foam. The region between the circles (spheres) is the portion occupied by the polymer. The spheres are empty.

in Section 14.1. The process of initiation is discussed in Chapter 21 of the textbook.[†] The cross-linked matrix is rigid. Once the polymer foam has formed, there is a need to remove the water and clean out the residual chemicals. The resulting material may be sliced into useful shapes.

Other polymers may be used to create carbon foams. For example, a foam made from polymethacrylonitrile (PMAN) with divinylbenzene serving as the cross-linker may be pyrolyzed to leave behind a carbon shell in the form of the original foam.

Interest has now expanded to low-density microcellular materials (LDMMs) composed of low-atomic-weight elements (e.g., C or Si polymers). They are porous and have uniform cell size, typically in the range 0.1 to 30 μm. They exhibit very low density, and because of the uniform cell size, the mechanical properties are homogeneous. An example is ultralow-density silica gel, which can have a density of 4 kg/m^3 — only three times that of air! These materials are both transparent and structurally self-supporting. They have promising applications as thermal or acoustical insulators.

W14.6 Porous Films

The sports world is enriched by the existence of garments made of breathable microporous films. These materials permit gases such as air and water vapor to pass through them readily while offering protection against water droplets. An example of such a porous film has the brand name Gore-tex, a Teflon-based material. Here the pores are generated by heat-casting a film sheet and stretching it, thereby expanding the preexisting defects until they form a connected network of pores. The pore sizes are typically 0.2 μm long and 0.02 μm wide. Water droplets cannot pass through the network because this would involve greatly expanding the droplets' surface area, and consequently the surface energy. Porosity levels of 40% are achievable.

[†] The material on this home page is supplemental to *The Physics and Chemistry of Materials* by Joel I. Gersten and Frederick W. Smith. Cross-references to material herein are prefixed by a "W"; cross-references to material in the textbook appear without the "W."

Recently, it was found that polypropylene contains two crystalline phases, an α-phase (monoclinic) and a β-phase (hexagonal), in addition to the amorphous phase.[†] The lower-density β-form (see Table 14.1) is less stable than the α-form and has a lower melting temperature. By applying stress to the material, it is possible to transform β to α. When this occurs there is a volume change, and void spaces are produced next to where the converted β-phase was. These voids percolate to form a network of pores. By adding fillers and rubbers into the pores and stretching the material it is possible to enlarge the pores to the optimal size.

Another way of preparing porous films is to irradiate the polymer film with high-energy ions. The ions create radiation damage as they penetrate the material, resulting in the breaking of polymer bonds along their tracks. By etching with acid or base, the damaged regions may be removed, leaving behind pores. Pore diameters as small as 20 nm may be produced by this technique.

W14.7 Electrical Conductivity of Polymers

It has been found experimentally that some polymers possess very high electrical conductivities when doped with small amounts of impurities. The electrical conductivities can approach those of copper [$\sigma_{Cu} = 58.8 \times 10^6 (\Omega \cdot m)^{-1}$ at $T = 295$ K; see Table 7.1]. An example of such a polymer is *trans*-polyacetylene doped with Na or Hg (n-doping) or I (p-doping). Other highly conducting polymers are polypyrrole $(C_4H_2NH)_n$, polythiophene $(C_4H_2S)_n$, polyaniline $(C_6H_4NH)_n$, and TTF-TCNQ (tetrathiafulvalene-tetracyanoquinodimethane). The conductivity tends to be highly anisotropic, with conductivity parallel to the polymer backbone strand being typically 1000 times larger than conductivity perpendicular to the strand. The precise origin of this high conductivity has been the subject of considerable debate.

Observe that strands of polyacetylene make almost perfect one-dimensional solids, with the molecule being typically 100,000 monomers in length. Furthermore, the covalent bonds comprising the polymer are energetically highly stable. Any doping of the sample proceeds by having donors or acceptor ions contribute carriers, without these ions actually entering the strands themselves. Since shielding is absent in a one-dimensional solid, these ions can be expected to interact with whatever mobile carriers may be present in the string via a long-range Coulomb force. As will be seen later, this is ineffective in backscattering the carriers, making the resistance of the polymer very small.

In Fig. W14.7, two bonding configurations are presented for the *trans* state of polyacetylene and also the *cis* configuration. Unlike the case of the benzene molecule, where a resonance structure is formed by taking a linear combination of the two bonding configurations, in long polymers each configuration maintains its distinct character. In benzene, the energy gap between the bonding and antibonding states is sufficiently large that the system relaxes into the bonding state. In polyacetylene the gap is very small. It is known that the carbon–carbon bond distances are different for the various bonding states: 0.12 nm for the triple bond (e.g., acetylene), 0.134 nm for the double bond (e.g., ethylene), and 0.153 nm for the single bond (e.g., ethane). By way of comparison, benzene has 0.140 nm, intermediate between the single- and double-bond values.

[†] P. Jacoby and C. W. Bauer, U.S. patent 4,975,469, Dec. 4,1990.

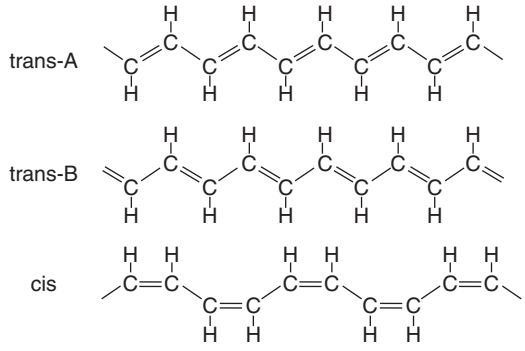

Figure W14.7. Two arrangements of the alternating single and double carbon–carbon bonds in polyacetylene, *trans*-A and *trans*-B. Also shown is the *cis* configuration.

The polyacetylene polymer may be modeled as a one-dimensional tight-binding dimerized chain with two carbon atoms (labeled A and B) per unit cell and unit cell length a. The amplitudes for having an electron reside on the nth A-atom site and the nth B-atom site will be denoted by A_n and B_n, respectively. The NN hopping integrals will be denoted by t and t' for the single- and double-bond distances, respectively. The details of the tight-binding equations are similar to those presented in Section 7.8, but extended here to the case of two atoms per unit cell. Thus

$$t'A_{n+1} + tA_n = \epsilon B_n, \tag{W14.61a}$$

$$tB_n + t'B_{n-1} = \epsilon A_n. \tag{W14.61b}$$

These equations may be simplified with the substitutions $A_n = \alpha \exp(inka)$ and $B_n = \beta \exp(inka)$, leading to

$$\epsilon\beta = (t + t'e^{ika})\alpha, \tag{W14.62a}$$

$$\epsilon\alpha = (t + t'e^{-ika})\beta. \tag{W14.62b}$$

This leads to the solution for the energy eigenvalues

$$\epsilon_\lambda(k) = \pm\sqrt{t^2 + t'^2 + 2tt'\cos(ka)}, \tag{W14.63}$$

where $\lambda = \pm$ and with the first Brillouin zone extending from $-\pi/a$ to π/a. There are two allowed energy bands separated by a gap. The allowed bands extend from $-|t + t'|$ to $-|t - t'|$ and from $|t - t'|$ to $|t + t'|$, respectively. The gap is from $-|t - t'|$ to $|t - t'|$. In virgin polyacetylene the lower band is filled and the upper band is empty. The material is a semiconductor, with a bandgap of 1.4 eV.

To describe the doping by an impurity atom (taken to be a donor, for the sake of definiteness), assume that the donor atom has an ionization energy E_d. The Hamiltonian for the chain-impurity system is

$$H = E_d|I\rangle\langle I| + \sum_{k,\lambda}[\epsilon_\lambda(k)|k, \lambda\rangle\langle k, \lambda| + V_\lambda(k)(|k, \lambda\rangle\langle I| + |I\rangle\langle k, \lambda|)], \tag{W14.64}$$

where $V_\lambda(k)$ governs the hopping back and forth between the donor ion and the polymer chain. The Schrödinger equation $H|\psi\rangle = \epsilon|\psi\rangle$ may be solved with a state of the form

$$|\psi\rangle = g|I\rangle + \sum_{k,\lambda} c_\lambda(k)|k, \lambda\rangle, \tag{W14.65}$$

and with the simplifying assumptions $\langle I|k, \lambda\rangle = 0$, $\langle I|I\rangle = 1$ and $\langle k'\lambda'|k\lambda\rangle = \delta_{\lambda,\lambda'}\delta_{k,k'}$. This leads to

$$E_d g + \sum_{k,\lambda} V_\lambda(k)c_\lambda(k) = \epsilon g, \tag{W14.66}$$

$$\epsilon_\lambda(k)c_\lambda(k) + gV_\lambda(k) = \epsilon c_\lambda(k). \tag{W14.67}$$

Solving the second equation for $c_\lambda(k)$ and inserting it into the first equation results in the eigenvalue equation

$$E_d + \sum_{k,\lambda} \frac{V_\lambda^2(k)}{\epsilon - \epsilon_\lambda(k)} = \epsilon. \tag{W14.68}$$

Assume that $V_\lambda(k) = V$ (independent of λ, k) and replace the sum over k states by an integral over the first Brillouin zone. Then

$$\begin{aligned} \epsilon - E_d &= \frac{V^2}{2\pi}\int_{-\pi/a}^{\pi/a} dk \frac{2\epsilon}{\epsilon^2 - t^2 - t'^2 - 2tt'\cos ka} \\ &= \frac{2V^2}{a}\frac{\epsilon}{\sqrt{(\epsilon^2 - t^2 - t'^2)^2 - 4t^2t'^2}}. \end{aligned} \tag{W14.69}$$

A graphical solution of the resulting sextic equation,

$$(\epsilon - E_d)^2[(\epsilon^2 - t^2 - t'^2)^2 - 4t^2t'^2] = \frac{4V^4\epsilon^2}{a^2}, \tag{W14.70}$$

shows that (at least) one discrete eigenstate will reside within the gap, irrespective of the location of E_d. This will be referred to as the *impurity level*. At $T = 0$ K this level is occupied.

For $T > 0$ K, electrons are donated to the polymer conduction band. (A similar description applies to holes contributed by acceptor dopants.) Resistance is brought about by the backscattering of these carriers by the charged impurity ions. Imagine that the electrons move along the z direction, the direction of alignment of the polymers. The distance of the impurity from the chain is denoted by D. The Coulomb potential presented by an ion at $z = 0$ is then $V(z) = -e/4\pi\epsilon_0\sqrt{z^2 + D^2}$. The matrix element for backscattering is, for $kD \gg 1$,

$$M = \langle\psi_f|V|\psi_i\rangle = -\frac{e^2}{4\pi\epsilon_0}\int_{-\infty}^{\infty}\frac{e^{2ikz}}{\sqrt{D^2 + z^2}}\,dz \longrightarrow -2\frac{e^2}{4\pi\epsilon_0}\sqrt{\frac{\pi}{4kD}}e^{-2kD}, \tag{W14.71}$$

which is seen to fall off rapidly for large values of kD. Thus the high mobility may be due, in part, to the small probability for backscattering events.

However, if the conduction in polyacetlyene is really one-dimensional, and electron–electron interactions are neglected, random scattering will serve to localize the electrons. The net result will be that it will be an insulator. More realistically, the electron–electron interaction is not negligible but is important. The electron–electron interaction serves to keep the electrons apart due to their Coulomb repulsion and lack of screening. This introduces strong correlations in the electronic motions and may override the tendency for localization.

Another approach to explaining the high conductivity of polyacetylene has to do with bond domain walls, called *solitons*. Imagine that one portion of the polymer chain is *trans*-A phase and a neighboring part is *trans*-B phase. This is illustrated in Fig. W14.8, which depicts the domain wall as an abrupt change in bonding configuration, a situation that is not energetically favorable. A lower-energy solution allows for the transition to take place more gradually, on a length scale on the order of 10 lattice constants. In a sense, one must introduce the concept of a partial chemical bond, making a transition from a single to a double bond over an extended distance. A more complete model, put forth by Su et al.[†] includes the elastic and kinetic energy of the lattice as well as the tight-binding Hamiltonian and a coupling between the phonons and the electrons. It may be shown that the undimerized chain (i.e., where there is only one atom per unit cell) is not the state of lowest energy, and a Peierls transition to the dimerized state occurs. This opens a gap at the Fermi level, as in the previous discussion, and makes the polymer a semiconductor rather than a metal. The spatial structure encompassing the foregoing transition from *trans*-A to *trans*-B, called a soliton, appears as a midgap discrete state. It is electrically neutral (i.e., the polymer is able to make the transition from *trans*-A to *trans*-B without the need to bring up or reject additional charge). However, it may be populated by donor electrons, as illustrated in Fig. W14.8.

The charged solitons may propagate along the chain and are difficult to scatter. Since the charge is spread out over an extended distance, it couples weakly to Coulomb scattering centers. The solitons consist of a correlated motion of the electron and the lattice and are similar in some ways to the polarons, familiar from three-dimensional solids. On the downside, however, the solitons may be trapped by defects and this can block their propagation. It is probably a fair statement to say that the final word on the mechanism responsible for the high conductivity of polyacetylene has not been fully decided upon.

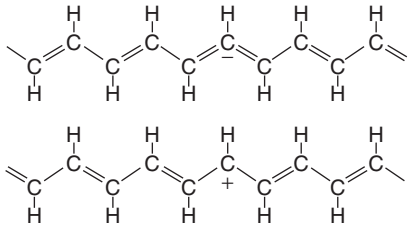

Figure W14.8. Domain walls between A and B phases of *trans*-polyacetylene.

[†] W. P. Su, J. R. Schrieffer, and A. J. Heeger, Solitons in Polyacetylene *Phys. Rev. Lett.*, **42**, 1698 (1979).

In some ways the situation in polyacetylene parallels that of the high mobility found for the modulation doping of GaAs–GaAlAs quantum-well structures (see Section W11.8). In the latter case the interface can be made nearly perfect, with electrons confined to move along the quantum well by the confining walls of the neighboring layers. Since the impurities do not reside in the wells, the Coulomb interaction is weaker and spread out over a large region of space. The impurities are not effective in scattering carriers, hence contributing to the high mobility.

W14.8 Polymers as Nonlinear Optical Materials

Optoelectronic devices are often based on nonlinear optical materials. As seen in Section 8.9, such a material is one in which the polarization vector (electric-dipole moment per unit volume) is a nonlinear function of the electric field of the light. One may make a power series expansion in the electric field(s) and write (employing the summation convention)

$$P_i(\omega) = \epsilon_0 \chi^{(1)}_{i,j}(\omega) E_j(\omega) + \epsilon_0 d^{(2)}_{i,j,k}(\omega; \omega_1, \omega_2) E_j(\omega_1) E_k(\omega_2) + \epsilon_0 d^{(3)}_{i,j,k,l}(\omega; \omega_1, \omega_2, \omega_3) E_j(\omega_1) E_k(\omega_2) E_l(\omega_3) + \cdots, \quad \text{(W14.72)}$$

where $d^{(2)}$ and $d^{(3)}$ are the second- and third-order nonlinear optical coefficients, respectively [see Eq. (8.46)]. For the case where $\omega_1 = \omega_2 = \omega/2$, the quantity $d^{(2)}$ determines the strength of second-harmonic generation (SHG), in which two photons of frequency $\omega/2$ may be combined to form a single photon of frequency ω. Similarly, when $\omega_1 = \omega_2 = \omega_3 = \omega/3$, the value of $d^{(3)}$ governs third-harmonic generation. The more general case of unequal photon frequencies covers various types of three- and four-wave mixing, as well as the dc Kerr effect, in which one of the photons has zero frequency.

For molecules with inversion symmetry, $d^{(2)}$ vanishes identically. Hence, for SHG in polymers, one must choose noncentrosymmetric molecules or solids. For efficient SHG the phase-matching condition must be satisfied; that is, photon energy and momentum must both be conserved:

$$\mathbf{k}_1 + \mathbf{k}_2 = \mathbf{k}, \qquad \omega_1 + \omega_2 = \omega, \quad \text{(W14.73)}$$

where $\omega = kc/n(\omega)$, $\omega_1 = kc/n(\omega_1)$, and $\omega_2 = kc/n(\omega_2)$, n being the index of refraction of the material. The goal is to design materials with as large values for the nonlinear susceptiblities as possible and to have these materials be thermally, mechanically, and chemically stable. These polymers may then be fashioned into fibers, sheets, or bulk material. The custom design of polymers, such as polydiacetylenes, has proved useful in attaining this goal.

To obtain high values for the nonlinear optical coefficients, use is made of the delocalized nature of the π electrons in hydrocarbon molecules. Generally, a "donor" group is placed at one end of a molecule and an "acceptor" group is placed at the other end. They are separated by a bridge region in which there are π electrons. This molecule is then incorporated into a polymer. The values of the susceptibilities depend on dipole matrix elements between electronic states and the differences of energies between these states. Generally, the larger the dipole matrix element, the larger the

susceptibility, and the closer an energy difference matches a photon energy, the larger the susceptibility. It is therefore expeditious to keep the donor group as far away from the acceptor as possible. A virtually excited electron from the donor makes a transition to the acceptor with a concurrent large value for the transition-dipole moment. In $d^{(2)}$ three dipole transitions and two energy denominators are involved. In $d^{(3)}$ there are four transitions and three denominators.

It is important for the various regions of the polymer to act coherently, and therefore it is important that there is alignment of the chain molecules. Since there is generally a static electric-dipole moment associated with the molecule, it may be aligned in an applied dc electric field, in a process called *poling*. The sample is heated above the glass-transition temperature, T_g, the material is poled, and then the temperature is lowered below T_g. The field is then removed and the sample has become an electret, with a net electric-dipole moment per unit volume. This itself has interesting applications in designing piezoelectric materials (in which a strain gives rise to an electric field, and vice versa) and electro-optic materials (in which the index of refraction may be altered by applying external electric fields). An example of a polymer that is used as a nonlinear optical material is 6FDA/TFDB. The molecule is shown in Fig. W14.9. An example of a nonlinear chromophore that may be adjoined to a polymer appears in Fig. W14.10 and is the 3-phenyl-5-isoxazolone compound.

One of the interesting features of polymers is the dependence of $d^{(3)}$ on the length of the chain ($\propto N^{3.5}$ for $N < 100$). This may be understood as follows. The end-to-end distance grows as N^{ν}, with $\nu \sim \frac{3}{5}$. One imagines a virtual excitation involving a "surface" state at the end of the chain. Since there are four transition moments entering $d^{(3)}$, this would give an exponent 4ν. Finally, there are N monomers per chain molecule, so a net exponent of $4\nu + 1 = 3.4$ could be expected. For very large polymers, however,

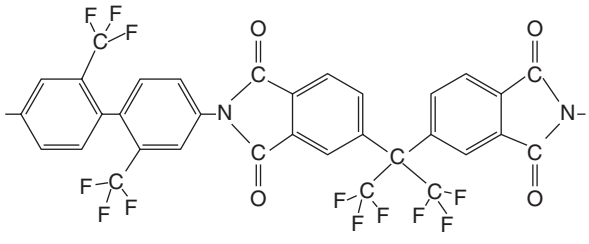

Figure W14.9. Monomer 6FDA/TFDB.

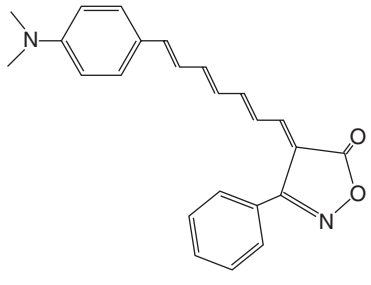

Figure W14.10. Chromaphore 3-phenyl-5-isoxazolone compound.

the dipole approximation would break down and higher frequency-dependent multipole moments would determine the nonlinear optical coefficients.

Recent attention has been directed to photorefractive polymers, such as doped poly(*N*-vinylcarbazole), for use as an optical information-storage material. The physics here is linear rather than nonlinear. A localized light beam directed at the polymer causes a real donor-to-acceptor transition of an electron. This produces a localized electric field that alters the local index of refraction. This constitutes the "write" step. A weak probe laser beam is able to detect the altered index of refraction in the "read" step. Poling in a strong external electric field restores the electrons to the donors, and thus the material is erasable. Since light is involved, one may attain several orders of magnitude greater read and write rates than with conventional magnetic media. By using two write lasers rather than one, it is possible to etch holographic interference patterns into the material.

PROBLEMS

W14.1 Consider a freely rotating chain consisting of N bonds, with the angle between successive bonds constrained to be equal to $\pi - \theta$.

(a) Show that $\langle \hat{u}_j \cdot \hat{u}_{j+k} \rangle = \cos^k \theta$.

(b) Show that the radius of gyration s is given by

$$s^2 = \frac{Na^2}{6} \frac{1 + \cos\theta}{1 - \cos\theta}.$$

W14.2 Show that the radius of gyration of a cyclic freely jointed chain is given by $s^2 = Na^2/12$.